

# Coexistence of charge density wave and spin-Peierls orders in quarter-filled quasi-one dimensional correlated electron systems

J. Riera<sup>a,b</sup> and D. Poilblanc<sup>a</sup>

<sup>a</sup>*Laboratoire de Physique Quantique & UMR-CNRS 5626, Université Paul Sabatier, F-31062 Toulouse, France*

<sup>b</sup>*Instituto de Física Rosario, Consejo Nacional de Investigaciones Científicas y Técnicas, y Departamento de Física, Universidad Nacional de Rosario, Avenida Pellegrini 250, 2000-Rosario, Argentina*

(October 11, 2018)

Charge and spin-Peierls instabilities in quarter-filled ( $n = 1/2$ ) compounds consisting of coupled ladders and/or zig-zag chains are investigated. Hubbard and t-J models including local Holstein and/or Peierls couplings to the lattice are studied by numerical techniques. Next nearest neighbor hopping and magnetic exchange, and short-range Coulomb interactions are also considered. We show that, generically, these systems undergo instabilities towards the formation of Charge Density Waves, Bond Order Waves and (generalized) spin-Peierls modulated structures. Moderate electron-electron and electron-lattice couplings can lead to a coexistence of these three types of orders. In the ladder, a zig-zag pattern is stabilized by the Holstein coupling and the nearest-neighbor Coulomb repulsion. In the case of an isolated chain, bond-centered and site-centered  $2k_F$  and  $4k_F$  modulations are induced by the local Holstein coupling. In addition, we show that, in contrast to the ladders, a small charge ordering in the chains, strongly enhances the spin-Peierls instability. Our results are applied to the  $\text{NaV}_2\text{O}_5$  compound (trellis lattice) and various phases with coexisting charge disproportionation and spin-Peierls order are proposed and discussed in the context of recent experiments. The role of the long-range Coulomb potential is also outlined.

PACS: 75.10.-b, 75.50.Ee, 71.27.+a, 75.40.Mg

## I. INTRODUCTION

Quasi-one dimensional correlated electrons systems at the commensurate filling of  $n = 1/2$  (quarter-filled band) show fascinating physical properties. A widely studied class of such materials are the so-called organics charge transfer salts like the Bechgaard salts [1]. These systems which consist of stacks of organics molecules forming weakly coupled one dimensional chains exhibit, at low temperature, a large variety of exotic phases such as superconducting, spin density wave, charge density wave (CDW) and spin-Peierls (SP) phases.

The vanadium inorganic compound  $\text{NaV}_2\text{O}_5$  is also believed to be a nearly perfect realization of a quarter-filled low dimensional system. Therefore, the nature of the SP phase [2,3] below  $T_{SP} \simeq 35\text{K}$  is expected to be quite different from the one occurring in the more conventional antiferromagnetic Heisenberg chain  $\text{CuGeO}_3$  (Ref. [4]).

The  $\text{NaV}_2\text{O}_5$  system is built from weakly coupled planes whose structure is shown in Fig. 1. It can be depicted as an array of parallel ladders (Fig. 1(b)) coupled in a trellis lattice. Note that a small buckling of the V plane can be neglected in first approximation. Oxygen atoms (not shown) are located at the center of the vertical and horizontal bonds of Fig. 1(a) and lead to effective hopping matrix elements and antiferromagnetic (AF) super-exchange interactions. LDA band structure calculations [5] and estimations based on empirical rules [6] lead to similar values of the hopping amplitudes along and perpendicular to the ladders,  $t_{\parallel} \simeq 0.15\text{eV}$  and  $t_{\perp} \simeq 0.35\text{eV}$  respectively. However, some controversy remains regarding the magnitude of the diagonal hop-

ping (see Fig. 1(c))  $t_{xy}$  with values ranging from 0.012eV (Ref. [5]) to 0.3eV (Ref. [6]).

Although the average valence of the vanadium in  $\text{NaV}_2\text{O}_5$  is 4.5 (half an electron per vanadium d-orbital on average), the exact nature of the charge ordering is still under active debate. Early X-rays diffraction experiments [7] were pointing in favor of a non-centrosymmetric structure implying two inequivalent vanadium sites. It was further suggested [7] that magnetic spin-1/2  $V^{4+}$  were forming one-dimensional (1D) chains separated by non-magnetic  $V^{5+}$  chains. Based on this assumption, various theoretical analyses of this material were attempted using dimerized Heisenberg chains [8] or spin-phonon models [9].

Recently, a new structure refinement at room temperature [10] suggested that, in contrast to earlier reports [7],  $\alpha'$ - $\text{NaV}_2\text{O}_5$  would have a centrosymmetric space group implying only one kind of vanadium site. Besides, below the transition temperature  $T_{SP}$ , joint neutron and X-ray diffraction experiments [11] reveal new superlattice reflections which can be ascribed to a lattice modulation associated to displacements of predominantly V atoms.

The insulating character of  $\text{NaV}_2\text{O}_5$  could, in fact, be simply understood in the framework of the quarter-filled Hubbard or t-J ladders [6,12,13] without invoking any charge order mechanism (as it is expected at room temperature). A simple analytic picture, valid when the hopping along the legs is small [6,12], gives a finite charge gap of the order of (for a very large Hubbard repulsion  $U$ ) the splitting  $2t_{\perp}$  between the bonding and antibonding states of the rungs. The existence of a metal-insulator transition in quarter-filled t-J ladder has been confirmed

by numerical calculations of the single particle density of state [12] and the charge gap [13] for realistic parameters. In the insulating state, the ground state (GS) configuration corresponds to the single occupancy of the bonding states on each rung and it has been argued that, in this case, the low-energy processes can be described by an effective AF Heisenberg chain [6,13], hence giving some relevance to earlier descriptions of this material [8,9]. Furthermore, angle-resolved photoemission data at room temperature [14] are consistent both with a description in term of an effective half-filled t-J chain [8] or in terms of a quarter-filled t-J ladder [12].

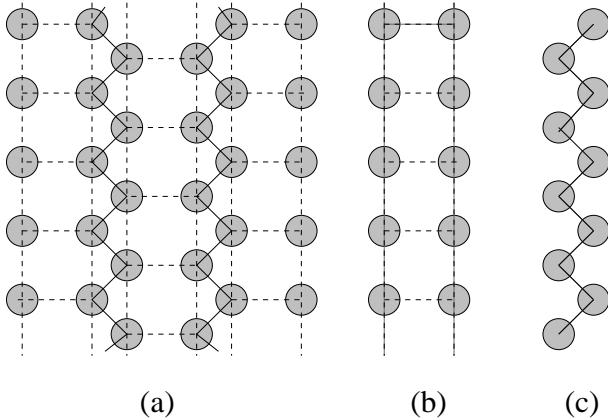


FIG. 1. (a) Structure of the vanadium planes of  $\text{NaV}_2\text{O}_5$  showing ladder (b) and chain (c) patterns. Each vanadium carries, on average, a charge of  $+0.5$ .

Recently, motivated by the experimental studies of  $\text{NaV}_2\text{O}_5$  at low temperature, charge ordering has been investigated theoretically [16,17,13,15]. It has been argued that repulsion between electrons on neighboring ladders can lead to charge disproportionations where the electrons are localized on a single leg of each ladder [13] (as in the original structure proposed in Ref. [7]) or form a zig-zag pattern within the ladder [16,17,15]. Although the Madelung energy, which includes also a long-range (LR) Coulomb interaction, slightly favors the chain charge ordering, it has been suggested [15] that, in contrast, the underlying coupling with the lattice could stabilize the zig-zag CDW. Experimental features in the optical conductivity at intermediate energies (0.6–2.5eV) [18] could be reproduced in a calculation of the t-J model on the trellis lattice [19] only by assuming an *ad-hoc* charge disproportionated GS, although low-energy charged magnons [18] could not be found.

In this paper, our aim is to investigate further, by numerical exact diagonalization (ED) techniques, the interplay between the electron-electron Coulomb repulsion and the electron-phonon (or spin-phonon) couplings. Indeed, charge disproportionation could come from a Holstein coupling, possibly related to the apical oxygen, as well as from a LR Coulomb repulsion. Although the emphasis is put here on the understanding of the physical

properties of  $\text{NaV}_2\text{O}_5$ , we believe our results can also be relevant for organic salts. The likely smallness of the interladder as well as many of the experimental results point to the possibility that the charge or SP instabilities are driven primarily by the ladder physics. [5,15] Thus, the first step of our analysis consists of the study of these structures by considering isolated quarter-filled t-J ladders including lattice-local charge couplings (Holstein) or modulations of the bond parameters (Peierls and SP couplings). We shall then try to determine whether the states found for the ladders are also consistent with the physics of the chains. Eventually, we shall consider the trellis lattice (Fig. 1(a)) of  $\text{NaV}_2\text{O}_5$  where the most likely states will be determined based on the previous results obtained for the individual ladder and zig-zag chain sublattices.

## II. ISOLATED LADDER: CHARGE INSTABILITY

We shall first consider the quarter-filled anisotropic t-J ladder (Fig. 1(b)) in the presence of an Holstein-coupling,

$$\begin{aligned}
 H &= H_{tJ} + H_V + H_H \quad (1) \\
 H_{tJ} &= J_{\parallel} \sum_{i,\alpha} (\mathbf{S}_{i,\alpha} \cdot \mathbf{S}_{i+1,\alpha} - \frac{1}{4} n_{i,\alpha} n_{i+1,\alpha}) \\
 &\quad + J_{\perp} \sum_i (\mathbf{S}_{i,1} \cdot \mathbf{S}_{i,2} - \frac{1}{4} n_{i,1} n_{i,2}) \\
 &\quad + t_{\parallel} \sum_{i,\alpha,\sigma} (\tilde{c}_{i,\alpha;\sigma}^{\dagger} \tilde{c}_{i+1,\alpha;\sigma} + h.c.) \\
 &\quad + t_{\perp} \sum_{i,\sigma} (\tilde{c}_{i,1;\sigma}^{\dagger} \tilde{c}_{i,2;\sigma} + h.c.) \\
 H_V &= V \sum_i (n_{i,1} n_{i+1,1} + n_{i,2} n_{i+1,2} + n_{i,1} n_{i,2}) \\
 H_H &= \sum_{i,\alpha} n_{i,\alpha} \delta_{i,\alpha} + \frac{1}{2} K \sum_{i,\alpha} \delta_{i,\alpha}^2,
 \end{aligned}$$

where  $\tilde{c}_{i,\alpha;\sigma}^{\dagger} = c_{i,\alpha;-\sigma} (1 - n_{i,\alpha;\sigma})$  are *hole* Guzwiller projected creation operators (the large on-site Coulomb interaction prevents doubly-occupancy) and the index  $\alpha$  stands for a chain index ( $= 1, 2$ ). We consider *a priori* different fermion hopping amplitudes ( $t_{\parallel}$ ,  $t_{\perp}$ ) or magnetic exchange interactions ( $J_{\parallel}$ ,  $J_{\perp}$ ) along the legs and along the rungs. Hamiltonian (1) can be viewed as the strong coupling limit of a Hubbard ladder so that one can assume a relation of the form  $J_{\parallel}/J_{\perp} = (t_{\parallel}/t_{\perp})^2$  between the parameters. A nearest neighbor (NN) Coulomb repulsion  $V$  has been included. Note that the electron-phonon coupling has been absorbed in the definition of the lattice displacement  $\delta_i$ . The magnitude of the coupling to the lattice is then given by a single parameter namely the inverse of the lattice stiffness  $1/K$ . The phonons have been given an infinite mass since the charge and spin dynamics are assumed here to involve smaller

time scales than lattice fluctuations (adiabatic approximation). Note that the on-site displacement  $\delta_i$  corresponds in fact to an effective parameter which might combine several effects. Physically, it could correspond to the displacement of the apical oxygen and/or to the displacements of the neighboring in-plane oxygen atoms toward or away from the V site.

Before proceeding with the study of Hamiltonian (1), it is instructive to recall the properties of the t-J ladder in the absence of electron-phonon coupling and NN repulsion. The electronic properties of this model at quarter filling have been investigated previously [6,12,13] and the existence of a metal-insulator transition has been shown [12,13]. It is believed that the system becomes insulating for (approximately)  $t_\perp > 2t_\parallel$ . Physically, this corresponds to the situation where the bonding and antibonding bands are completely separated, the lower band becoming effectively half-filled so that an arbitrary small repulsion opens a charge gap. This physical situation might be relevant for the insulating phase of the NaV<sub>2</sub>O<sub>5</sub> material.

Although the lattice is considered here in the adiabatic approximation, no supercell order is assumed *a priori* and the lowest energy equilibrium lattice configuration is obtained through a self-consistent procedure (as in the rest of the paper). Indeed, the total energy functional  $E(\{\delta_{i,\alpha}\})$  can be minimized with respect to the sets of distortions  $\{\delta_{i,\alpha}\}$  by solving the non-linear set of local coupled equations,

$$K\delta_{i,\alpha} + \langle n_{i,\alpha} \rangle = 0, \quad (2)$$

where  $\langle \dots \rangle$  is the GS mean value obtained by ED (using the Lanczos algorithm) of Hamiltonian (1). Since the second term depends implicitly on the distortion pattern  $\{\delta_{i,\alpha}\}$ , Eqs. (2) can be solved by a regular iterative procedure. [20]

The phase diagram of the Holstein-t-J ladder model is shown in Fig. 2(a) for a realistic set of parameters. These results have been obtained by studying  $2 \times 6$  and  $2 \times 8$  clusters. In the absence of NN repulsion  $V$ , a rapid transition occurs from a uniform phase (U) at small coupling (or equivalently large lattice rigidity) to a localized phase at large coupling. This strong coupling phase is characterized by a charge ordering with two types of (almost) completely empty or completely occupied sites arranged in some disordered patterns. More interestingly, a CDW phase with a “zig-zag” arrangement of the excess charge (which exists also for  $V = 0$  only in a very narrow region around  $1/K \sim 2.5$ ) is stabilized by the NN repulsion  $V$ . In contrast to the localized phase, the charge disproportionation in this zig-zag CDW state is not complete. Notice that there is a finite critical value of  $1/K$  associated to the stability of the CDW phase. This feature might be due to the fact that the uniform ladder for  $1/K = 0$  is, for an anisotropy ratio of  $t_\parallel/t_\perp = 0.4$ , already in an insulating state with a charge gap (see Ref. [12]).

### III. ISOLATED LADDER: COEXISTING CHARGE AND SP ORDERS

The possibility of a coexisting SP order in the previous CDW state can be studied by considering additional Peierls and SP couplings realized by making the following substitutions in Hamiltonian (1);

$$t_\parallel \rightarrow t_\parallel(1 + \delta_{i,\alpha}^B), \quad (3)$$

$$J_\parallel \rightarrow J_\parallel(1 + g\delta_{i,\alpha}^B), \quad (4)$$

and by adding a new elastic term  $\frac{1}{2}K_B \sum_{i,\alpha} (\delta_{i,\alpha}^B)^2$ .

Note that the spin-Peierls order is, for a quarter-filled band, intrinsically linked to a bond order wave (BOW) characterized by a modulation of the hopping amplitudes [21] as given by Eq. (3). In other words, the expectation values  $\langle c_{i,\alpha;\sigma}^\dagger c_{i+1,\alpha;\sigma} \rangle$  and  $\langle \mathbf{S}_{i,\alpha} \cdot \mathbf{S}_{i+1,\alpha} \rangle$  should exhibit similar modulations along the legs. For simplicity, we shall assume here that the magnetic exchange interaction  $J_\parallel$  involves two virtual hops  $t_\parallel$  so that one can take, in first approximation,  $g \simeq 1$ . However, the qualitative results of this study do not depend on the choice of  $g$ . It should be noticed in addition that we shall consider modulations only along the legs of the ladders since our analysis showed that modulations of the rungs were not favored.

Since our purpose is to investigate the role of the additional Peierls coupling on the zig-zag CDW state, we shall first consider an *ad-hoc* effective potential,

$$H_{\text{eff}} = V_{\text{eff}} \sum_{i,\alpha} (-1)^{(x_{i,\alpha} + y_{i,\alpha})} n_{i,\alpha}, \quad (5)$$

replacing the terms  $H_H + H_V$  in Hamiltonian (1) in order to stabilize the zig-zag pattern. Qualitatively, this term mimics the combined effects of the Holstein lattice coupling and the NN Coulomb repulsion. The previous method based on Eq. (2) can be extended here to deal with the lattice-bond interaction. The lowest energy configuration is found by minimizing the GS energy with respect to the full set of parameters  $\{\delta_{i,\alpha}^B\}$ . This is achieved by solving exactly, using the same iterative procedure as before, the set of non-linear equations,

$$K_B \delta_{i,\alpha}^B + gJ_\parallel \langle \mathbf{S}_{i,\alpha} \cdot \mathbf{S}_{i+1,\alpha} - \frac{1}{4} n_{i,\alpha} n_{i+1,\alpha} \rangle + t_\parallel \langle \tilde{c}_{i,\alpha;\sigma}^\dagger \tilde{c}_{i+1,\alpha;\sigma} + h.c. \rangle = 0. \quad (6)$$

on finite clusters. As shown in the phase diagram of Fig. 2(b), a finite value of the coupling strength  $1/K_B \sim 2$  is needed to produce a dimerized pattern overimposed to the CDW state. Above this critical value, a finite modulation of the form  $\delta_{i,\alpha}^B = \delta^B (-1)^{x_{i,\alpha}}$  (the ladder is oriented along the x-axis) appears simultaneously with the CDW order parameter for any  $V_{\text{eff}}$ . As can be seen in Fig. 3(a), the charge disproportionation,  $\Delta n = |\langle n_i \rangle - \frac{1}{2}|$ ,

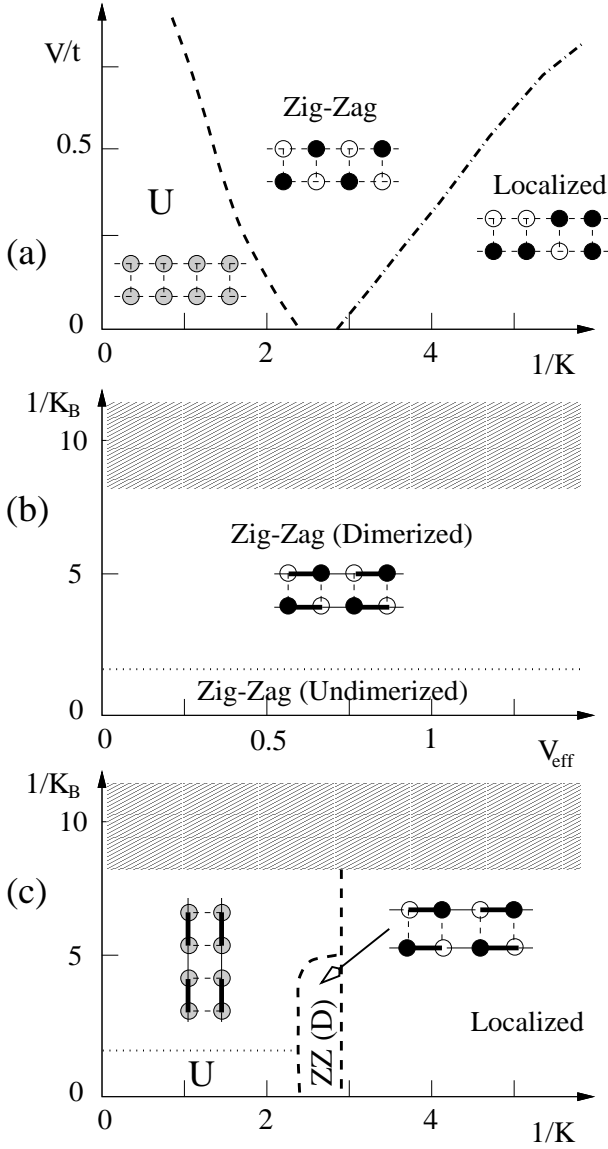


FIG. 2. Typical phase diagrams of  $\frac{1}{4}$ -filled anisotropic t-J ladders (a) as a function of the NN Coulomb repulsion  $V$  and the on-site Holstein coupling of strength  $1/K$ ; (b) as a function of the Peierls lattice coupling and the effective potential  $V_{\text{eff}}$ ; (c) as a function of Holstein and Peierls lattice couplings. These results have been obtained by ED of small clusters with anisotropy ratios  $t_{\parallel}/t_{\perp} = 0.4$  and  $J_{\parallel}/J_{\perp} = 0.16$ . Shaded regions are unphysical (see text).

increases almost linearly with the magnitude of the effective potential and depends weakly on the magnetoelastic coupling as expected. On the other hand, the amplitude  $\delta_B$  of the dimerization (Fig. 3(c)) increases strongly with  $1/K_B$  when  $1/K_B > 2$ . However, for very strong couplings, our method gives an unphysical solution  $\delta_B > 1$  (implying ferromagnetic bonds) shown by a shaded region in Fig. 2(b) (as in the rest of the paper). This signals that our simple initial model breaks down for such a strong coupling with the lattice and that other terms

should be included (quartic terms, etc...). Interestingly enough, the presence of a zig-zag charge pattern is not at all required to observe a dimerization in the ladder. On the contrary, as it is clear in Fig. 3(c), the dimerization occurs for  $V_{\text{eff}} = 0$  (i.e. for a uniform distribution of the charge) and is even weakly *suppressed* by  $V_{\text{eff}}$ .

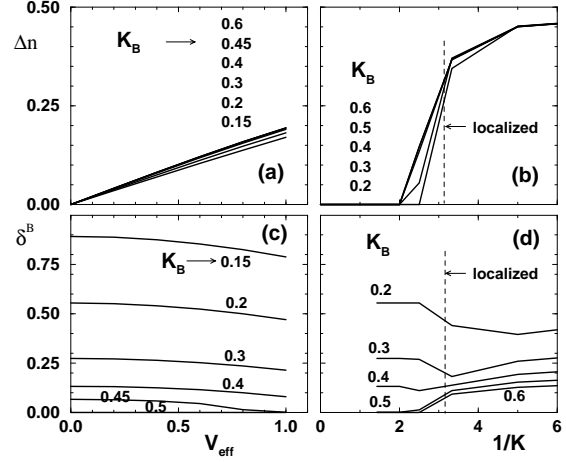


FIG. 3. CDW order parameter  $\Delta n$  (a,b) and bond modulation  $|\delta_i^B|$  (c,d) of a  $\frac{1}{4}$ -filled t-J ladder for various lattice bond stiffness  $K_B$  (as indicated on the plots). (a,c) as a function of the effective potential  $V_{\text{eff}}$ ; (b,d) as a function of the on-site Holstein coupling strength  $1/K$ . In the “localized” phase (on the right of the dashed line), estimates based on an average over the system are shown. These results have been obtained by ED of small clusters with anisotropy ratios  $t_{\parallel}/t_{\perp} = 0.4$  and  $J_{\parallel}/J_{\perp} = 0.16$ .

We now turn to the investigation of the full Hamiltonian including both Holstein and Peierls-like lattice couplings, the amplitudes of each of them being characterized by the two independent coupling constants  $1/K$  and  $1/K_B$  respectively. The GS configuration for the site and bond deformations can be obtained exactly on small clusters by solving simultaneously, by the previous recursive method, the two sets of non-linear equations (2) and (6). As before, at each step of the recursive procedure, the quantum mechanical Hamiltonian is diagonalized by using a Lanczos algorithm. Our results, for the same set of parameters  $t_{\mu}$ ,  $J_{\mu}$  as above, are summarized in the phase diagram of Fig. 2(c) with the corresponding behaviors of the local CDW order parameter and bond deformation shown in Figs. 3(b,d). In contrast to the previous model, no zig-zag CDW ordering appears at small Holstein coupling  $1/K$ . A uniform dimerized (D) phase is stable for large enough  $1/K_B$ . It is important to notice that the dimerized zig-zag (D-ZZ) phase is found only in a narrow region located around  $1/K \sim 2.5$  while a larger Holstein coupling stabilizes a localized phase (with no well-defined periodic pattern). In addition, these data suggest that the Peierls coupling rather tends to suppress the charge

order and hence to destabilize the D-ZZ phase with respect to the D phase. However, the region of stability of the D-ZZ phase (of particular interest in the case of the  $\text{NaV}_2\text{O}_5$  material) is expected to be greatly enhanced by a NN Coulomb repulsion (see Fig. 2(a)) as we have checked numerically.

#### IV. ISOLATED CHAIN: CHARGE INSTABILITY

As mentioned above, in  $\text{NaV}_2\text{O}_5$ , the ladders are coupled by diagonal bonds forming zig-zag chains. Besides, as mentioned in the Introduction, many quasi-1D molecular compounds contains weakly coupled chains. Therefore, we shall now consider the role of the Holstein and Peierls lattice couplings on one-dimensional chains. For completeness, we start with a 1D Hubbard model at quarter-filling ( $n = 1/2$ ) coupled with an on-site (classical) phonon field,

$$H = t \sum_{i,\sigma} (c_{i,\sigma}^\dagger c_{i+1,\sigma} + h.c.) + U \sum_i n_{i,\uparrow} n_{i,\downarrow} + V \sum_i n_i n_{i+1} + \sum_i n_i \delta_i + \frac{1}{2} K \sum_i \delta_i^2. \quad (7)$$

At quarter-filling, the Fermi wave vector is given by  $q_{2k_F} = \frac{\pi}{2}$  so that, at small  $U$ , one expects an instability towards a  $2k_F$ -CDW state of wavevector  $\lambda_{2k_F} = 4a$  ( $a$  is the lattice spacing) mediated by the electron-phonon coupling. In contrast, for large  $U$ , the system becomes more similar to a gas of interacting spinless fermions and the instability is likely to occur at wavevector  $2k_F^{SF} = 4k_F$ . More generally, we can parametrize the charge density as, [21]

$$\langle n_i \rangle = \frac{1}{2} + A_{2k_F} \cos(2\pi \frac{r_i}{4a} + \Phi_{2k_F}) + A_{4k_F} \cos(2\pi \frac{r_i}{2a} + \Phi_{4k_F}). \quad (8)$$

A schematic phase diagram is shown in Fig. 4(a) for  $V = 0$ . The uniform  $U$  metallic phase ( $A_{2k_F} = A_{4k_F} = 0$ ) is restricted to a region at small electron-phonon coupling. Above a critical line  $1/K$  vs  $U$ , three different insulating CDW phases can be distinguished; (i) at small  $U$ , a  $2k_F$ -CDW phase ( $A_{4k_F} \simeq 0$ ) centered on the sites, i.e. with  $\Phi_{2k_F} = 0$ ; (ii) at intermediate  $U$  (in the range 4–8), a *bond*-centered  $2k_F$ -CDW phase i.e. with  $\Phi_{2k_F} = \frac{\pi}{4}$ ; (iii) at large  $U$ , a  $4k_F$ -CDW ( $A_{2k_F} \simeq 0$ ,  $\Phi_{4k_F} = 0$ ). As seen in Fig. 4(b), a small NN repulsion suppresses completely the intermediate phase and enlarges the region of stability of the  $4k_F$ -CDW phase [22].

We now restrict ourselves to the strong electron correlation limit ( $t$ - $J$  model) to discuss further the role of the NN repulsion  $V$ . Besides, since in  $\text{NaV}_2\text{O}_5$  the zig-zag chains form part of the trellis lattice we include NNN hopping matrix elements  $t'$  and exchange integrals  $J'$

which correspond to the interactions along the legs of the ladders. Hence, the Hamiltonian is,

$$H = H_{tJ} + H_V + H_H \quad (9)$$

$$H_{tJ} = J \sum_i (\mathbf{S}_i \cdot \mathbf{S}_{i+1} - \frac{1}{4} n_i n_{i+1}) + t \sum_{i,\sigma} (\tilde{c}_{i,\sigma}^\dagger \tilde{c}_{i+1,\sigma} + h.c.) + J' \sum_i (\mathbf{S}_i \cdot \mathbf{S}_{i+2} - \frac{1}{4} n_i n_{i+2}) + t' \sum_{i,\sigma} (\tilde{c}_{i,\sigma}^\dagger \tilde{c}_{i+2,\sigma} + h.c.)$$

$$H_V = V \sum_i n_i n_{i+1}$$

$$H_H = \sum_i n_i \delta_i + \frac{1}{2} K \sum_i \delta_i^2.$$

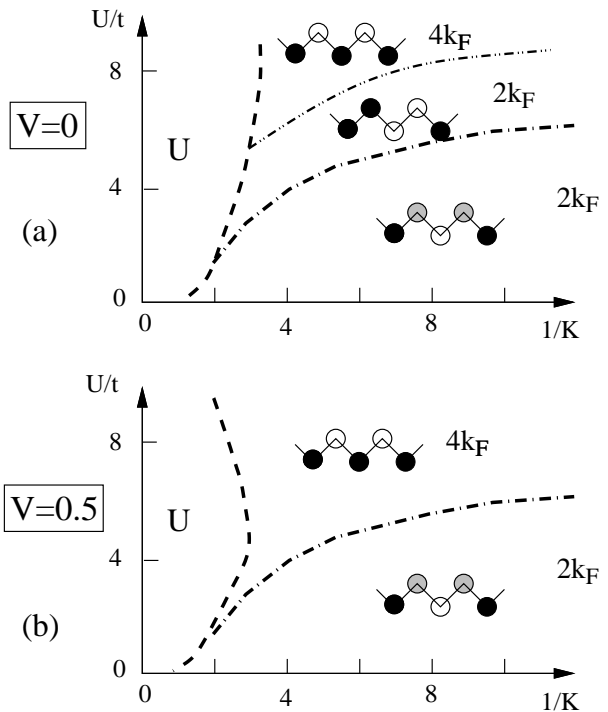


FIG. 4. Typical phase diagrams of a  $\frac{1}{4}$ -filled Hubbard chain in the presence of an on-site Holstein coupling without (a) or with a nearest neighbor Coulomb repulsion  $V$  (b) obtained from ED of small periodic chains.

The phase diagram of Fig. 5(a) corresponding to the  $J' = t' = 0$  case confirms the stabilization of the  $4k_F$  charge order by the repulsion  $V$ . It can be seen that, similarly to what happens in the  $t$ - $J$  ladder case (Fig. 2(a)), there is a phase of charge disproportionation occurring in the region of large Peierls coupling  $K^{-1}$ , with a definite pattern. Some important qualitative changes in the phase diagram are introduced by the NNN hoppings and exchange interactions  $t'$  and  $J'$  as seen in Fig. 5(b) with the appearance of the bond-centered  $2k_F$ -CDW phase stable at intermediate Holstein coupling. As in the Hubbard chain, this phase is suppressed by an intermediate NN Coulomb repulsion  $V$ .

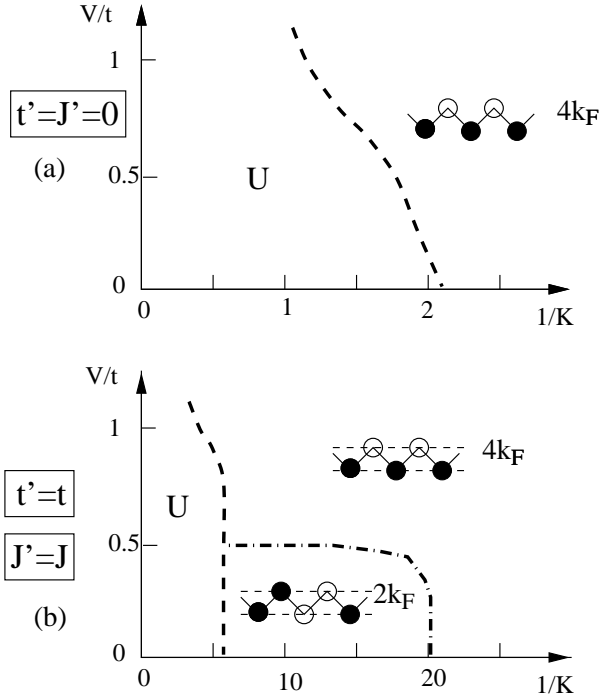


FIG. 5. Typical phase diagrams of a  $\frac{1}{4}$ -filled  $t$ - $J$  chain for  $J = 0.3$  as a function of the NN repulsion  $V$  and the strength of the on-site Holstein coupling  $1/K$  obtained from ED of small periodic chains. A hopping  $t' = t$  and a magnetic exchange  $J' = J$  between NNN sites have been included (omitted) in (b) (in (a)).

## V. TRELLIS LATTICE: CHARGE INSTABILITY

At this stage, it is interesting to apply our results (valid, strictly speaking, in the case of *isolated* chains or ladders) to investigate the possibility of charge ordering in the 2D trellis lattice of  $\text{NaV}_2\text{O}_5$  (see Fig. 1(a)). Obviously, the type of order the most likely to appear depends whether the chains or the ladders are the main structures of this compound. Since the interladder couplings, although still not well determined, are quite likely to be smaller than the couplings along the rungs of the ladders it is to be expected that the physics of the ladders is going to dominate the behavior of the trellis lattice. However, this possibility has not been proven so far. Thus, here we shall rather try to determine the most probable 2D order *compatible* with both the chain and the ladder physics. A  $4k_F$  charge order in the zig-zag chains would imply the 2D formation of parallel chains of average charge  $0.5 + \Delta n$  and  $0.5 - \Delta n$ . This corresponds to the structure originally proposed by Galy and coworkers [7] (assuming a complete disproportionation  $\Delta n = 0.5$ ). However, experimental evidences accumulate in favor of a modulation of the charge also in the  $x$  direction of the ladder legs, hence more compatible with the  $2k_F$ -CDW orders in the zig-zag chains with NNN couplings. Two typical patterns exhibiting bond-centered or

site-centered CDW along the zig-zag chains are shown in Figs. 6(a) and 6(b) respectively. Note that only the structure of Fig. 6(a) is fully compatible with the zig-zag CDW ordering in *all* the ladders. Based on our previous studies, we believe this structure should be stable in the 2D trellis lattice for large on-site Coulomb repulsion  $U$ , intermediate short-range Coulomb repulsion and when the hoppings and magnetic couplings along the legs ( $J_{\parallel} = J'$ ,  $t_{\parallel} = t'$ ) exceed the cross-bond terms  $J_{xy}$  and  $t_{xy}$  (corresponding to  $J$  and  $t$  in the chain model). It is interesting to notice that, in our picture, the charge ordering is not saturated ( $\Delta n < 0.5$ ). However, a doubling of the periodicity occurs in the direction of the ladders for any finite value of the order parameter  $\Delta n$  consistently with recent experiments [11].

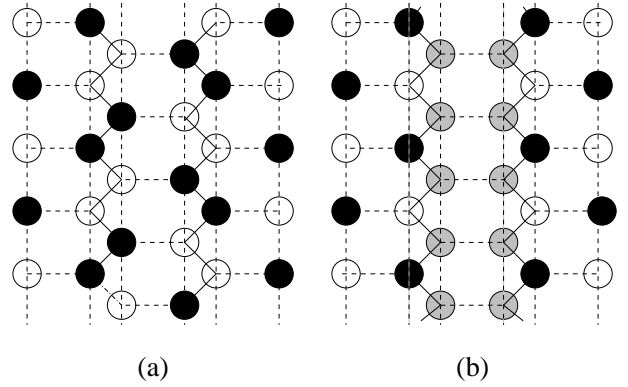


FIG. 6. Typical patterns of charge ordering on the  $\text{NaV}_2\text{O}_5$  lattice structure showing a supercell of 4 sites along the zig-zag chain. The filled (open) symbols correspond to an excess (depression) of charge compared to the average charge of  $1/2$  (grey sites have a density close to the average density). (a) Bond-centered charge density wave of period 4 ( $Q = 2k_F$ ) with two types of non-equivalent sites. (b) Site-centered charge density wave of period 4 ( $Q = 2k_F$ ) with three types of non-equivalent sites.

So far, only short range Coulomb repulsion has been considered. We briefly comment on the role of the long range Coulomb repulsion. We have done simple classical calculations of the Madelung energy corresponding to the various charge configuration introduced before. As previously mentioned, most charge ordered states have lower energies than the uniform state. Therefore, we believe that the long range part of the Coulomb repulsion should increase further the tendency towards charge disproportionation.

## VI. ISOLATED CHAIN: COEXISTING CHARGE AND SP ORDERS

We now proceed with the investigation of the last issue, namely the role of an additional Peierls coupling in the chains. We shall follow a method similar to the one used

before for the ladder structure. For simplicity, we use an effective potential to stabilize the bond-centered  $2k_F$ -CDW phase found previously (see Fig. 5(b)),

$$H_{\text{eff}} = V_{\text{eff}} \sum_i n_i \cos(2\pi \frac{r_i}{4a} + \frac{\pi}{4}). \quad (10)$$

replacing the terms  $H_V + H_H$  of Hamiltonian (9). This effective potential can also include the effects of the LR Coulomb interaction on the trellis lattice discussed in the previous section. The amplitude of the CDW can then be tuned by  $V_{\text{eff}}$ . We first consider a Peierls coupling introduced in the NN bonds by the following substitutions,

$$t \rightarrow t(1 + \delta_i^B), \quad (11)$$

$$J \rightarrow J(1 + 2\delta_i^B), \quad (12)$$

where the corresponding elastic energy has the usual form  $\frac{1}{2}K_B \sum_i (\delta_i^B)^2$ . GS properties are obtained by solving iteratively the set of non-linear equations,

$$K_B \delta_i^B + 2J \langle \mathbf{S}_i \cdot \mathbf{S}_{i+1} - \frac{1}{4} n_i n_{i+1} \rangle + t \langle \tilde{c}_{i;\sigma}^\dagger \tilde{c}_{i+1;\sigma} + h.c. \rangle = 0. \quad (13)$$

Typical phase diagrams are shown in Figs. 7(a) and 7(b) for a simple  $t$ - $J$  chain and a  $t$ - $t'$ - $J$ - $J'$  chain respectively. Interestingly enough, a spin-Peierls instability (with the same periodicity  $\lambda_{2k_F} = 4a$  as the underlying CDW) occurs for arbitrary small coupling  $1/K_B$ . This phase is characterized by three types of bonds in the 4-sites unit cell; weak (W), strong (S) or intermediate (I) bonds depending on the magnitudes of  $\delta_i^B$ . The sequence I-S-W-S in the  $t' = J' = 0$  case corresponds in fact to a mixture with a  $4k_F$  component. Note that, in the absence of  $V_{\text{eff}}$  and for  $1/K_B > 1$ , a simple dimer phase of sequence W-S-W-S (pure  $4k_F$  component) is stable. As expected, the external potential generates an additional  $2k_F$  component whose magnitude increases with  $V_{\text{eff}}$ . It is interesting to mention here that similar orders occur e.g. in quasi-1D organic conductors such as the SP compound (TMTTF)<sub>2</sub>PF<sub>6</sub>; while the metallic phase is dimerized, a quadrupling of the unit cell is observed in the low temperature insulating phase. On the other hand, in the case of the zig-zag chain with NNN couplings, an almost pure single-Fourier ( $2k_F$ ) CDW is observed with a S-I-W-I sequence (Figs. 7(b)). It is important here to stress that, in contrast to the ladder case studied previously, the SP order occurs only in the presence of charge ordering. Furthermore, the SP order parameter follows closely the magnitude of the charge disproportionation as it is clear from Figs. 8(a) and 8(c).

For completeness, we should also assume in the zig-zag chain the possibility of an additional Peierls coupling acting on the bonds connecting NNN sites. This effect is then characterized by a new set of bond variables  $\{\delta_i^{B'}\}$  and a different elastic constant  $K'_B$ . In the real materials, these new parameters are not completely independent from the previous ones. However, since the exact

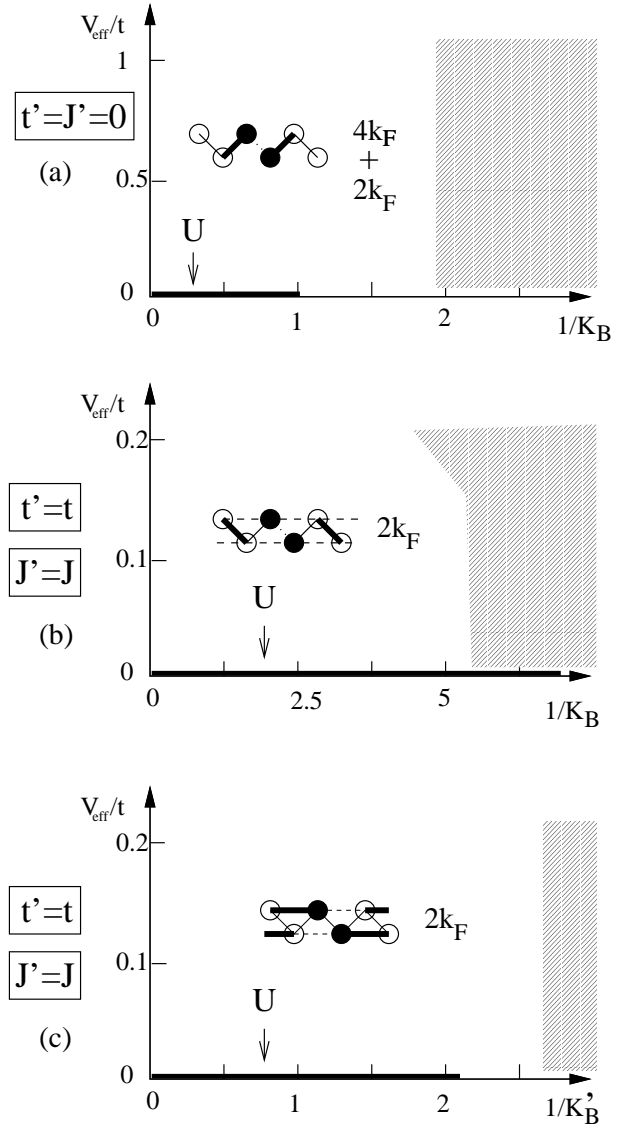


FIG. 7. Typical phase diagrams of a  $1/4$ -filled  $t$ - $J$  chain for  $J = 0.3$  as a function of the effective potential  $V_{\text{eff}}$  (see text) and the strength of the Peierls bond couplings  $1/K_B$  and  $1/K'_B$  obtained from ED of small periodic chains. A hopping  $t'$  and a magnetic exchange  $J'$  between NNN sites have been included (resp. omitted) in (b) and (c) (resp. in (a)). In (a) and (b) (resp. (c)) the Peierls coupling is included only on the bonds connecting NN sites (resp. NNN sites).

relations between them, which depend on very fine details of the chemistry of the material, are quite difficult to determine, we shall here examine the role of this new coupling separately from the previous one. It will be easy then to add the two effects afterwards, at least at a qualitative level. We then consider the following substitution,

$$t' \rightarrow t'(1 + \delta_i^{B'}), \quad (14)$$

$$J' \rightarrow J'(1 + 2\delta_i^{B'}), \quad (15)$$

for the parameters associated to the bonds connecting the NNN sites  $i$  and  $i + 2$ .

The set of local equations,

$$K'_B \delta_i^{B'} + 2J' \langle \mathbf{S}_i \cdot \mathbf{S}_{i+2} - \frac{1}{4} n_i n_{i+2} \rangle + t' \langle \tilde{c}_{i;\sigma}^\dagger \tilde{c}_{i+2;\sigma} + h.c. \rangle = 0. \quad (16)$$

have been solved as before on small 12 or 16 sites periodic chains and the results are summarized in the phase diagram shown on Fig. 7(c). For any arbitrary small SP coupling, a dimerization occurs in the two parallel chains formed by the NNN bonds, coexisting with the underlying CDW state. As seen in Figs. 8(b) and 8(d), two qualitatively different regimes have to be distinguished; (i) for small SP couplings (let say  $1/K'_B < 2$ ), the dimerization and the charge order appear simultaneously and follow a linear behavior as a function of the magnitude of the external potential; (ii) for larger couplings, the mixed CDW-SP state is stable even in the absence of  $V_{\text{eff}}$ . In that case, the charge disproportionation  $\Delta n$  is further increased by  $V_{\text{eff}}$  while the dimerization  $\delta^B$  remains almost constant. It is important to stress here that, in both regimes, both order parameters follow a very similar behavior as a function of the coupling constants of the model suggesting that the two types of orders are intrinsically linked.

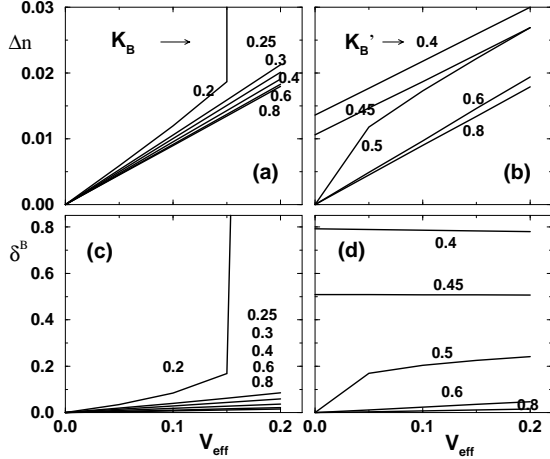


FIG. 8. CDW order parameter  $\Delta n$  [in (a) and (b)] and bond modulation  $|\delta_i^B|$  [in (c) and (d)] of a  $\frac{1}{4}$ -filled t-J chain for  $J = 0.3$  as a function of the effective potential  $V_{\text{eff}}$  (see text) and for various lattice stiffness  $K_B$  (as indicated on the plots) obtained from ED of small periodic chains. A hopping  $t'$  and a magnetic exchange  $J'$  between NNN sites have been included. In (a) and (c) (resp. (b) and (d)) the Peierls coupling is included on the bonds connecting NN sites (resp. NNN sites).

## VII. TRELLIS LATTICE: COEXISTING CHARGE AND SP ORDERS

Based on our previous studies of the coexistence of CDW and SP orders in isolated ladders and zig-zag

chains, we shall now attempt to construct a unified picture for the 2D trellis lattice of  $\text{NaV}_2\text{O}_5$ . Although this approach is not rigorous, we believe it can provide reliable qualitative predictions of the low temperature structure of this material. Our starting point is the charge ordered pattern of Fig. 6, likely to be stabilized by a local on-site Holstein coupling and/or a LR Coulomb repulsion. As seen before, this structure combines the zig-zag CDW pattern of the ladders and the bond-centered  $2k_F$ -CDW of the chains. If the SP instability is driven primarily by a Peierls coupling in the diagonal bonds  $t_{xy} \equiv t$  and  $J_{xy} \equiv J$ , one should expect the pattern of Fig. 9(a) with the I-S-W-S sequence along the zig-zag chains. However, as argued previously, the stability of the bond-centered  $2k_F$ -CDW in the chains which we assume here requires rather sizable NNN couplings  $t'$  and  $J'$  corresponding to the  $t_{\parallel}$  and  $J_{\parallel}$  parameters of the trellis lattice. Therefore, we believe that the Peierls coupling corresponding to these bonds can no longer be neglected. In this case, one can argue that the structure shown in Fig. 9(b) is more stable than the one shown in Fig. 9(a). It is obtained by a superposition of the two types of SP orders of the t-t'-J-J' chains shown in Figs. 7(b) and 7(c), each of them being mediated by Peierls couplings in the diagonal bonds and the legs respectively. This state is characterized by a dimerization in the legs and a modulation S-I-W-I in the t-t'-J-J' chain. Note that the SP order on the diagonal bonds of the t-t'-J-J' chain is somehow “locked” to the charge order i.e. the weak (W) bonds are always the ones connecting two sites with an excess of charge and so on. However, the actual pattern of the

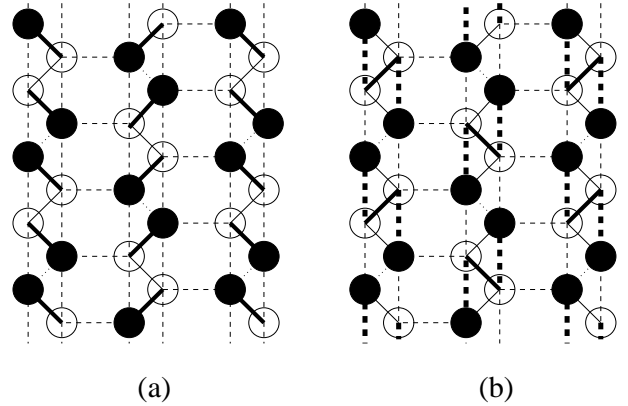


FIG. 9. Typical patterns of coexisting lattice distortion and charge ordering on the  $\text{NaV}_2\text{O}_5$  lattice structure showing a periodicity of 4 sites along the t-t'-J-J' chain. The filled (open) symbols correspond to an excess (depression) of charge compared to the average charge of  $1/2$ . These patterns show a modulation of the bond exchange couplings along the zig-zag chain with three types of bonds and two types of sites ( $2k_F$  order of the charge density). Thick, thin and dotted lines correspond to strong, intermediate and weak bonds respectively. (a) Mixed  $2k_F$ - $4k_F$  lattice distortion. (b)  $2k_F$  lattice distortion.



chains depends on the relative phase between the two SP modulations. Fig. 6(b) corresponds to the simplest and most natural choice with only two different kinds of triangles. Besides, we believe that this possibility has the lowest energy.

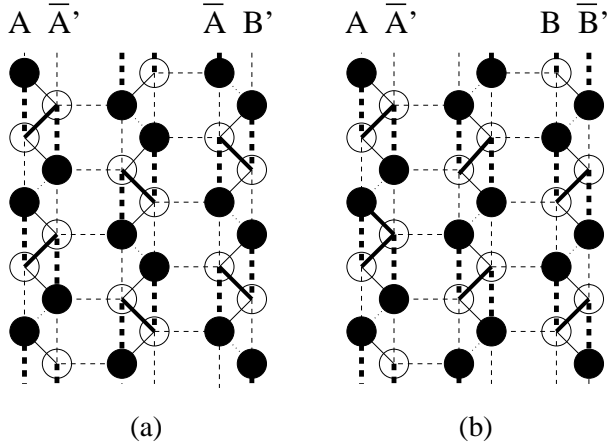


FIG. 10. Same distortion and charge ordering pattern along the zig-zag chains as on Fig. 9(b) but with a doubling of the periodicity in the transverse direction. A quadrupling (doubling) of the 2D unit cell occurs in (a) ((b)).

The last step in our procedure consists now to refine the final structure using our knowledge of the SP instabilities in an isolated ladder. In fact, by examining the ladders of Fig. 9(b), we realize that the type of dimerization occurring in the legs do not correspond to any type of SP order found before in the isolated ladder. However, although still imposing a fixed type of pattern in the legs and zig-zag chains, other arrangements are possible in the transverse direction leading to qualitatively different structures. Since the charge ordering doubles the periodicity in the ladder direction, there are two different configurations A and B of the ladder legs, which transform into each other by a translation of a unit vector. In addition, due to the coexisting SP-BOW order, a reflection with respect to a site perpendicularly to the leg leads to two non-equivalent configurations  $\bar{A}$  and  $\bar{B}$ . As can be seen straightforwardly, the characteristic pattern of the zig-zag chains of Fig. 9(b), can appear in four different ways (all related to each other by a lattice translation and/or a reflection with respect to a site), namely  $AA'$ ,  $\bar{A}\bar{B}'$ ,  $\bar{B}A'$  and  $B\bar{B}'$  (the prime refers to the second leg). Various orders can be realized by arbitrary sequences in the transverse direction involving different configurations in each primitive cell. Note that each primitive cell contains two zig-zag chains but the pattern in the second zig-zag chain is somehow imposed its two neighboring ones. The previous arrangement shown in Fig. 9(b) corresponds then to a periodic arrangement in the transverse direction like  $-AA'-AA'-$  (equivalent to e.g.  $-\bar{B}\bar{B}'-\bar{B}\bar{B}'-$  and so on). In contrast, the ordering patterns of Figs. 10(a) and 10(b) of the form  $-AA'-\bar{A}\bar{B}'-$  (equivalent to  $-AA'-\bar{B}A'-$

$B\bar{B}'-$  respectively double the periodicity in the transverse direction as well. It is important to stress that only the pattern shown in Fig. 10(b) show the expected mixed CDW-SP ordering of the D-ZZ type in *all* the ladders (see phase diagrams in Figs. 2(b) and (c)). We can then argue that the ordering shown in Fig. 10(b) can be stabilized both by the couplings in the chains and in the ladders. This state corresponds in fact to a check-board pattern with a doubling of the unit cell and is consistent with recent light and neutron scattering experiments [11].

## VIII. CONCLUSIONS

To summarize, the role of Holstein and Peierls electron-phonon couplings as well as magneto-phonon (SP) couplings has been investigated in the adiabatic approximation in quarter-filled one-dimensional chain and ladder systems. A numerical method based on ED techniques supplemented by a self-consistent procedure has been used to determine various phase diagrams as a function of the strengths of the lattice couplings. We have shown that, generically, CDW, BOW and spin-Peierls orders coexist in such systems. Moreover, in many cases, the SP instability is enhanced by a charge disproportionation. Eventually, we have considered the case of the trellis lattice of  $\text{NaV}_2\text{O}_5$ . Based on the previous results for isolated chains and ladders, we have proposed a mixed CDW-BOW-SP ground state with a zig-zag charge pattern in the ladders and a modulated bond structure involving 7 different bonds. Such ordered state doubles the unit cell introducing a check-board type pattern.

Whether the charge ordering and the BOW-SP transition occur simultaneously at the same temperature is not yet clear but could be resolved experimentally by thermodynamical measurements. In addition, such transitions should have different spectroscopic signatures due to profound changes in the GS excitation spectrum. On one hand, charge ordering is expected to strongly enhance the charge gap (although the insulating character of the material at high temperature could be accounted for by a local on-site repulsion alone). On the other hand, the opening of a spin gap should be associated to the SP-BOW transition.

Very recent X-ray diffuse scattering studies of  $\text{NaV}_2\text{O}_5$  [23] suggest that 3D structural fluctuations are important above the transition and, hence, that transverse interactions (other than magnetic) should be important to stabilize the ordered phase. In our description, the SP mechanism is intrinsically linked to the occurrence of charge ordering, possibly induced by a coupling with the 3D lattice (treated here in the adiabatic approximation). Therefore, we believe that the mechanism proposed in the present work is, to some degree, weakly dependent on the actual magnetic couplings of the trellis lattice, which, so far, are not precisely known.

## IX. ACKNOWLEDGEMENTS

D. P. and J. R. thank IDRIS, Orsay (France) for allocation of CPU time on the C94 and C98 Cray supercomputers. J. R. acknowledges partial support from the Ministry of Education (France) and the Centre National de la Recherche Scientifique.

- 
- [1] For reviews on Bechgaard salts see e.g. D. Jérôme and H. J. Schulz, *Adv. Phys.* **31**, 299 (1982); D. Jérôme, *Organic Superconductors* (Dekker, New York, 1994). T. Ishiguro and K. Yamaji, Springer Series Solid State Vol. 88 (Springer Verlag, Berlin, 1990).
  - [2] M. Isobe and Y. Ueda, *J. Phys. Soc. Jpn* **65**, 1178 (1996); Y. Fujii et al. *J. Phys. Soc. Jpn* **66**, 326 (1997); M. Weiden et al., *Z. Phys. B* **103**, 1 (1997).
  - [3] For ultrasonic evidence of the SP transition in  $\text{NaV}_2\text{O}_5$  see e.g. P. Fertey, M. Poirier, M. Castonguay, J. Jegoudez, and A. Revcolevschi, *Phys. Rev. B* **57**, 13698 (1998).
  - [4] For a review on  $\text{CuGeO}_3$ , see e.g. J. P. Boucher and L. P. Regnault, *J. Phys. I (Paris)* **6**, 1939 (1996).
  - [5] H. Smolinski, C. Gros, W. Weber, U. Peuchert, G. Roth, M. Weiden, C. Geibel, *Phys. Rev. Lett.* **80**, 5164 (1998).
  - [6] P. Horsch and F. Mack, preprint cond-mat/9801316.
  - [7] A. Carpy and J. Galy, *Acta Cryst. B* **31**, 1481 (1975).
  - [8] D. Augier, D. Poilblanc, S. Haas, A. Delia and E. Dagotto, *Phys. Rev. B* **56**, R5732 (1997).
  - [9] David Augier and Didier Poilblanc, *Eur. Phys. J. B* **1**, 19 (1998); D. Smirnov, P. Millet, J. Leotin, D. Poilblanc, J. Riera, D. Augier and P. Hansen, *Phys. Rev. B* **57**, R11035 (1998); For treatment of non-adiabatic phonons in SP systems see also D. Augier, D. Poilblanc, E. Sorensen, I. Affleck, preprint cond-mat/9802053, to be published in *Phys. Rev. B*; G. Wellein, H. Fehske, A.P. Kampf, preprint cond-mat/9804085.
  - [10] A. Meetsma, J. L. de Boer, A. Damascelli, T. T. M. Palstra, J. Jegoudez and A. Revcolevschi, *Acta. Cryst.*, in press (1998); H.-G. von Schnering, R. Kremer, O. Jepsen, T. Chatterji and M. Weiden, preprint (1997).
  - [11] Tapan Chatterji, K. D. Liss, G. J. MacIntyre, M. Weiden, R. Hauptmann and G. Geibel, preprint (1998). Note that these authors also point out that only a single  $V$  site of average valence 4.5 exists at room temperature in agreement with Ref. [10].
  - [12] J. Riera, D. Poilblanc and E. Dagotto, preprint cond-mat/9804209, to be published in *Eur. Phys. J. B*.
  - [13] S. Nishimoto and Y. Ohta, preprint cond-mat/9805336.
  - [14] K. Kobayashi, T. Mizokawa, A. Fujimori, M. Isobe, and Y. Ueda, *Phys. Rev. Lett.* **80**, 3121 (1998).
  - [15] M. V. Mostovoy and D. I. Khomskii, preprint cond-mat/9806215.
  - [16] H. Seo and H. Fukuyama, preprint cond-mat/9805185.
  - [17] P. Thalmeier and P. Fulde, preprint cond-mat/9805230.
  - [18] A. Damascelli *et al.*, *Phys. Rev. Lett.* **81**, 918 (1998).
  - [19] S. Nishimoto and Y. Ohta, preprint cond-mat/9808061; See also T. Ohama, H. Yasuoka, M. Isobe and Y. Ueda, preprint (1998).
  - [20] A. Dobry and J. Riera, *Phys. Rev. B* **56**, 2912 (1997); see also F. Schönfeld, G. Bouzerar, G.S. Uhrig and E. Müller-Hartmann, preprint cond-mat/9803084.
  - [21] Coexistence between BOW and CDW has been discussed, in the context of charge transfer salts, in e.g. K. C. Ung, S. Mazumdar and D. K. Campbell, *Solid St. Commun.*, **85**, 917 (1993); K. C. Ung, S. Mazumdar and D. Toussaint, *Phys. Rev. Lett.* **73**, 2603 (1994).
  - [22] For  $U = \infty$  (half-filled spinless fermion model), a transition from the (uniform) metallic phase to a ( $4k_F$ -CDW) insulating phase occurs, even in the absence of any electron-phonon interaction, at  $V = 2$ ; See F. D. M. Haldane, *J. Phys. C* **14**, 2585 (1981).
  - [23] S. Ravy, J. Jegoulez and A. Revcolevschi, preprint cond-mat/9808313.